Science Translational Medicine
AAAS

A Human Disease Model of Drug Toxicity–Induced Pulmonary Edema in a Lung-on-a-Chip Microdevice

Dongeun Huh *et al.*

Sci Transl Med **4**, 159ra147 (2012);
DOI: 10.1126/scitranslmed.3004249

Editor's Summary

Pulmonary Edema-on-a-Chip

Drug testing in animal models is time-consuming, costly, and often does not accurately predict the adverse effects in humans. Toward a more reliable output, Huh and colleagues developed a "lung-on-a-chip" that models human lung function in both normal and disease states.

The authors cultured two types of human lung cells in parallel microchannels, which were separated by a thin membrane. Much like the human lung, the upper "alveolar" channel was filled with air, whereas the lower "microvascular" channel was filled with liquid. Vacuum was cyclically applied to the sides of the channels to mimic the breathing motion of the lung. When Huh and colleagues added interleukin-2 (IL-2) to the microvascular channel, the fluid started to leak into the air compartment. This process reproduces what is seen in the clinic, where IL-2 induces pulmonary leakage, also known as "edema." Cyclic mechanical strain introduced with IL-2 compromised the pulmonary barrier even further and led to a threefold increase in leakage. As expected, the addition of angiopoietin-1 stabilized the endothelial junctions and inhibited IL-2 –induced vascular leakage. Lastly, the authors tested their pulmonary disease model against a new pharmacological agent, GSK2193874, which blocks certain ion channels activated by mechanical strain. This drug inhibited leakage, suggesting that it would be a viable treatment option for patients with pulmonary edema who are being mechanically ventilated.

Huh *et al.* have recreated the human lung on a microfluidic chip and shown that it not only mimics lung function in response to IL-2 and mechanical strain but also successfully predicts the activity of a new drug for pulmonary edema. The beneficial effects of GSK2193874 still need to be confirmed in humans, but were preliminary validated in animals in a study by Thorneloe *et al.* (this issue). The next step is to hook this lung up to other chip-based organs––heart, liver, pancreas, etc.––with the goal of one day being able to rapidly screen many drugs and conditions that could affect patient health.

Science Translational Medicine (print ISSN 1946-6234; online ISSN 1946-6242) is published weekly, except the last week in December, by the American Association for the Advancement of Science, 1200 New York Avenue NW, Washington, DC 20005.

BIOENGINEERING

A Human Disease Model of Drug Toxicity–Induced Pulmonary Edema in a Lung-on-a-Chip Microdevice

Dongeun Huh,[1,2,3] Daniel C. Leslie,[1,2] Benjamin D. Matthews,[2,4] Jacob P. Fraser,[1] Samuel Jurek,[2] Geraldine A. Hamilton,[1] Kevin S. Thorneloe,[5] Michael Allen McAlexander,[6] Donald E. Ingber[1,2,7]*

Preclinical drug development studies currently rely on costly and time-consuming animal testing because existing cell culture models fail to recapitulate complex, organ-level disease processes in humans. We provide the proof of principle for using a biomimetic microdevice that reconstitutes organ-level lung functions to create a human disease model-on-a-chip that mimics pulmonary edema. The microfluidic device, which reconstitutes the alveolar-capillary interface of the human lung, consists of channels lined by closely apposed layers of human pulmonary epithelial and endothelial cells that experience air and fluid flow, as well as cyclic mechanical strain to mimic normal breathing motions. This device was used to reproduce drug toxicity–induced pulmonary edema observed in human cancer patients treated with interleukin-2 (IL-2) at similar doses and over the same time frame. Studies using this on-chip disease model revealed that mechanical forces associated with physiological breathing motions play a crucial role in the development of increased vascular leakage that leads to pulmonary edema, and that circulating immune cells are not required for the development of this disease. These studies also led to identification of potential new therapeutics, including angiopoietin-1 (Ang-1) and a new transient receptor potential vanilloid 4 (TRPV4) ion channel inhibitor (GSK2193874), which might prevent this life-threatening toxicity of IL-2 in the future.

INTRODUCTION

The development of safe and effective drugs is currently hampered by the poor predictive power of existing preclinical animal models that often lead to failure of drug compounds late in their development after they enter human clinical trials. Given the tremendous cost of drug development and the long timelines involved, major pharmaceutical companies and government funding agencies, including the U.S. Food and Drug Administration (FDA), National Institutes of Health (NIH), Defense Advanced Research Projects Agency (DARPA), and Defense Threat and Reduction Agency (DTRA), are now beginning to recognize a crucial need for new technologies that can quickly and reliably predict drug safety and efficacy in humans in preclinical studies.

One approach to meeting this challenge is the development of three-dimensional cell cultures in which cells are grown within extracellular matrix (ECM) gels to induce expression of more tissue-specific functions (*1*). These models are currently being used for testing drug efficacy and toxicities; however, they fail to provide organ-level functionalities (molecular transport across tissue-tissue interfaces, contributions of vascular and airflow, etc.) that are required for the development of meaningful disease models. A potential solution to this problem is the development of human "organs-on-chips" in which microscale engineering technologies are combined with cultured living human cells to create microfluidic devices that recapitulate the physiological and mechanical microenvironment of whole living organs (*2*–*10*). These organomimetic microdevices enable the study of complex human physiology in an organ-specific context, and more importantly, they offer the potential opportunity to develop specialized in vitro human disease models that could revolutionize drug development (*2*, *11*–*15*). However, human organ-on-chip models that effectively mimic complex disease processes and drug responses have not yet been developed.

We recently microengineered a "lung-on-a-chip" that reconstituted the alveolar-capillary interface of the human lung and exposed it to physiological mechanical deformation and flow; in other words, it breathed rhythmically much like a living lung (*4*). Although this microengineered system recapitulated organ-level physiological functions, including pulmonary vascular barrier integrity and inflammatory responses to pathogens, it has not yet been shown to mimic complex human disease processes or to predict human responses to pharmaceutical agents at clinically relevant doses. Thus, this state-of-the-art system failed to provide the proof of principle required by the pharmaceutical industry and regulatory agencies to prove that organs-on-chips can be used to create human-relevant disease models that have potential to replace preclinical animal experiments.

Here, we explored whether we can use the human lung-on-a-chip microdevice to develop a microengineered disease model of pulmonary edema in human lungs, which is a life-threatening condition characterized by abnormal accumulation of intravascular fluid in the alveolar air spaces and interstitial tissues of the lung due to impaired homeostatic fluid balance mechanisms that lead to vascular leakage across the alveolar-capillary barrier (*16*–*18*). This disease can result from increased capillary hydrostatic pressure or microvascular permeability produced by various cardiovascular, respiratory, renal, and neurological diseases (*16*–*20*) or by dose-limiting drug toxicities. For example, systemic administration of interleukin-2 (IL-2) for the treatment of malignant melanoma and metastatic renal cell carcinoma is limited by toxicities that induce microvascular inflammation and injury leading to extravasation and accumulation of fluid in the alveolar air spaces (*21*–*24*), as well as activation of the coagulation

[1]Wyss Institute for Biologically Inspired Engineering at Harvard University, Boston, MA 02115, USA. [2]Vascular Biology Program, Departments of Pathology and Surgery, Children's Hospital Boston and Harvard Medical School, Boston, MA 02115, USA. [3]Department of Biomedical Engineering, College of Medicine, Seoul National University, Seoul 110-744, Korea. [4]Department of Medicine, Children's Hospital Boston, Boston, MA 02115, USA. [5]Heart Failure Discovery Performance Unit, Metabolic Pathways and Cardiovascular Therapy Area Unit, GlaxoSmithKline, King of Prussia, PA 19406, USA. [6]Respiratory Therapy Area Unit, GlaxoSmithKline, King of Prussia, PA 19406, USA. [7]School of Engineering and Applied Sciences, Harvard University, Cambridge, MA 02138, USA.
*To whom correspondence should be addressed. E-mail: don.ingber@wyss.harvard.edu

cascade leading to intra-alveolar fibrin deposition (*25*, *26*) (Fig. 1A). Here, we focused on establishing a human lung disease model on-chip that reconstitutes these toxic side effects of IL-2 and resultant pulmonary edema in patients. We also investigated the possibility that mechanical breathing motions might contribute to pulmonary toxicity of IL-2 and tested whether therapeutics such as angiopoietin-1 (Ang-1) and a new inhibitor of transient receptor potential vanilloid 4 (TRPV4), GSK2193874 (GlaxoSmithKline), can suppress pulmonary vascular leakage in this in vitro human disease model, and hence have the potential to treat human patients.

RESULTS

Mimicking pulmonary edema in the human lung-on-a-chip

To explore whether we could mimic the dose-limiting toxicity of IL-2 in vitro, we used a lung-on-a-chip microfluidic device made of an optically transparent silicone elastomer that contains closely apposed layers of human alveolar epithelial and pulmonary microvascular endothelial cells cultured in two parallel microchannels separated by a thin (10 μm), porous, flexible membrane coated with ECM (*4*) (Fig. 1B). In the upper channel, the alveolar epithelium was exposed to air to mimic the alveolar air space; culture medium was flowed through the microvascular channel; and cyclic vacuum was applied to hollow side chambers to cyclically stretch the tissue layers (10% cyclic strain at 0.2 Hz) and thus reproduce physiological breathing movements (Fig. 1B).

To develop a drug toxicity–induced human pulmonary edema model on-chip, we perfused a clinically relevant dose of IL-2 (1000 U/ml) through the microvascular channel of this device. Phase-contrast microscopic imaging revealed that clear liquid began to leak across the endothelium lining the microvascular channel and into the previously air-filled alveolar compartment, initially accumulating preferentially in a meniscus at the sides of the channel (Fig. 1C). This leakage occurred continuously over a period of 4 days, causing a progressive reduction in the volume of the air space until the entire alveolar microchannel became completely flooded (Fig. 1C). Moreover, when we introduced IL-2 and physiological concentrations of the human blood plasma proteins—prothrombin and fluorescently labeled fibrinogen—into the microvascular channel, we observed extensive formation of fluorescent fibrin clots on the apical surface of the alveolar epithelium (Fig. 1, D and E, and movie S1). These clots also were organized as porous, fibrous, network structures (Fig. 1F), confirming that they mimic natural fibrin clots. Clot formation is likely due to activation of factor X to Xa by tissue factor expressed or released by inflamed cells during IL-2–induced leakage of plasma proteins into the alveolar space, which then cleaves prothrombin to thrombin, which acts as a procoagulant to convert fibrinogen to fibrin (*27*).

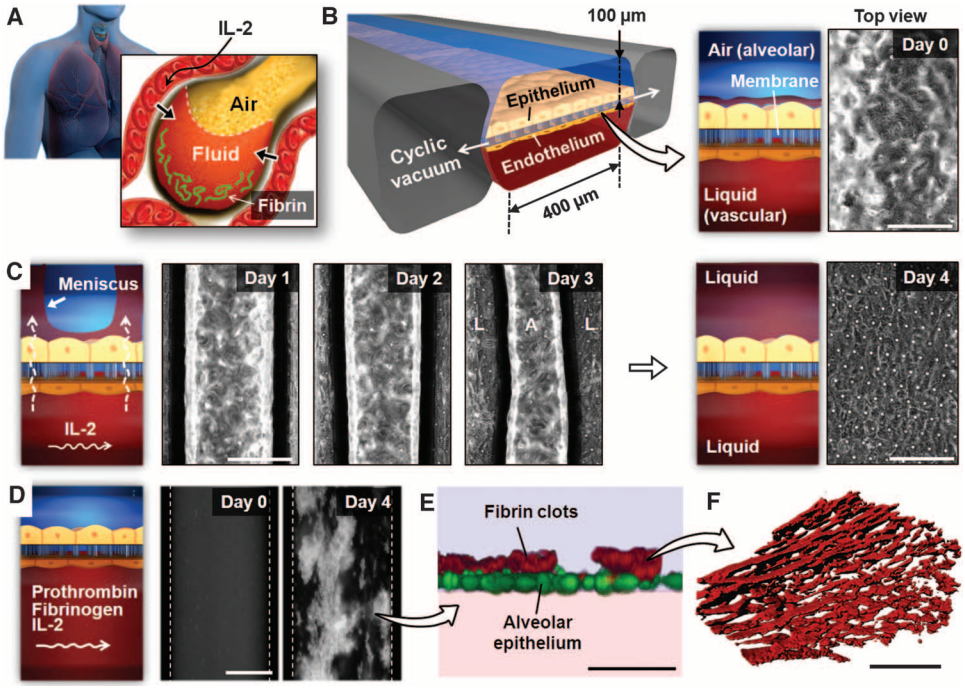

Fig. 1. A microengineered model of human pulmonary edema. (**A**) IL-2 therapy is associated with vascular leakage that causes excessive fluid accumulation (edema) and fibrin deposition in the alveolar air spaces. (**B**) IL-2–induced pulmonary edema is modeled in a microengineered lung-on-a-chip that reproduces the lung microarchitecture and breathing-induced cyclic mechanical distortion of the alveolar-capillary interface. The top "air" portion is the alveolar channel; the bottom "liquid" portion is the vascular channel. The phase-contrast image shows a top-down view of the apical surface of the alveolar epithelium maintained at an air-liquid interface in the upper microchannel. Scale bar, 200 μm. (**C**) Endothelial exposure to IL-2 (1000 U/ml) causes liquid in the lower microvascular channel to leak into the alveolar chamber (days 1 to 3) and eventually fill the entire air space (day 4). The meniscus between air (A) and liquid (L) appears as dark bands in the phase-contrast images. Scale bars, 200 μm. (**D**) During IL-2 treatment, prothrombin (100 μg/ml) and fluorescently labeled fibrinogen (2 mg/ml) introduced into the microvascular channel form fluorescent fibrin clots (white) over the course of 4 days. Dotted lines represent channel walls. Scale bar, 200 μm. (**E**) A fluorescence confocal microscopic image shows that the fibrin deposits (red) in (D) are found on the upper surface of the alveolar epithelium (green). Scale bar, 50 μm. (**F**) The clots in (D) and (E) are highly fibrous networks, as visualized at high magnification by confocal fluorescence microscopy. Images are representative of three independent experiments. Scale bar, 5 μm.

Pathological changes in barrier integrity

We then quantitatively examined these pathological changes in lung fluid transport by measuring the permeability of the microengineered alveolar-capillary barrier to fluorescein isothiocyanate (FITC)–conjugated inulin that had been injected into the microvascular channel (Fig. 2A). The fluorescence intensity of fluids collected from the alveolar compartment was monitored during endothelial exposure to IL-2. In the absence of cyclic mechanical strain, a gradual increase in fluorescence was detected over time, which was small but significant (Fig. 2B). However, when the tissue

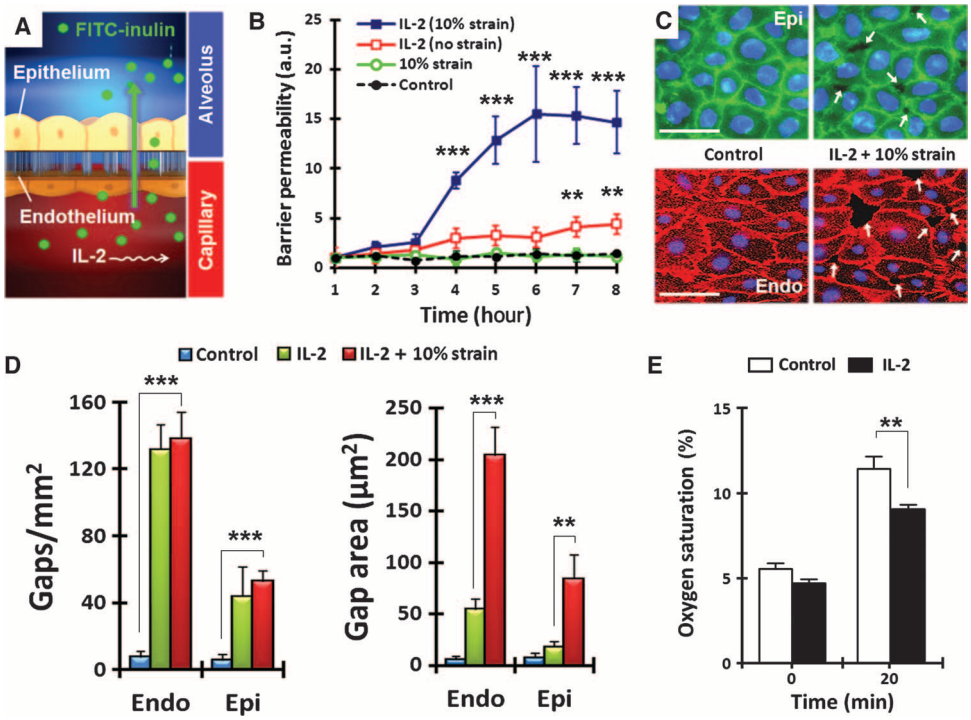

Fig. 2. Quantitative analysis of pulmonary edema progression on-chip. (**A**) Pathological alterations of barrier function were quantified by measuring alveolar-capillary permeability to FITC-inulin (green) introduced into the microvascular channel containing IL-2. (**B**) Barrier permeability in response to IL-2, with and without cyclic strain. Error bars indicate SEM; data from three experiments were normalized to the mean at time 0. a.u., arbitrary units. (**C**) Immunostaining of epithelial occludin (green) and vascular endothelial cadherin (VE-cadherin; red) after 3 days of cyclic stretch with 10% strain without IL-2 (control) or with IL-2. White arrows indicate intercellular gaps; blue, nuclear staining. Scale bars, 30 μm. (**D**) Compromised barrier integrity due to IL-2 and mechanical strain was assessed by quantifying the number and size of intercellular gaps. (**E**) Quantification of O_2 uptake from air in the epithelial channel by deoxygenated medium flowing through vascular channel in control and IL-2–treated lung chips. (B and E) Data are means ± SEM (n = 3). $^{**}P < 0.01$, $^{***}P < 0.001$ (B, D, and E).

layers were subjected to mechanical deformations that mimicked physiological breathing movements, the same dose of IL-2 severely compromised pulmonary barrier function and further increased tissue permeability by more than threefold within 8 hours (Fig. 2B). We have previously demonstrated that mechanical stretch alone does not have any detrimental effects on barrier integrity in this system, regardless of its duration (*4*).

Immunostaining of intercellular junctions revealed that administration of IL-2 in conjunction with physiological mechanical strain disrupted cell-cell junctions and resulted in the formation of multiple paracellular gaps in both the epithelial and endothelial monolayers relative to controls (Fig. 2, C and D). When compared to the effects of IL-2 alone, application of physiological cyclic mechanical strain (10% at 0.2 Hz) during IL-2 treatment did not affect the number of the gaps but significantly increased their size (area) by about fourfold (Fig. 2D). Thus, these results reveal an important new contributor to the development of vascular leakage and pulmonary edema during IL-2 therapy that has not been identified in previous studies (*28*, *29*): Mechanical forces generated by breathing motions act in synergy with IL-2 to enhance opening of cell-cell junctions in both the alveolar epithelium and capillary endothelium.

Effects on gas transport across the alveolar-capillary barrier

The leakage of fluid from the vascular channel to the air space induced by IL-2 treatment possibly compromised oxygen transport in our microdevice, as occurs in humans with pulmonary edema. To investigate these effects, we perfused the vascular channel with deoxygenated medium (by bubbling 95% N_2 and 5% CO_2 through the medium reservoir), exposed the air space to room air (~20% O_2), and measured the O_2 concentration in the medium using an in-line fluorescent sensor. Perfusion of the deoxygenated medium through control (untreated) lung chips for 20 min under these conditions resulted in a more than twofold increase in oxygenation of the medium, whereas the lung chip treated with IL-2 for 4 days significantly compromised O_2 uptake by the flowing medium (Fig. 2E). Thus, this on-chip human disease model also mimics an important physiological consequence of pulmonary edema related to impaired gas exchange in the lung.

Drug testing on-chip

Next, we explored whether this human pulmonary edema-on-a-chip model can be used to identify pharmacological agents that might prevent vascular leakage induced by IL-2. We first tested Ang-1, which has been shown to stabilize endothelial intercellular junctions (*30*), and found that coadministration of Ang-1 (100 ng/ml) with IL-2 in the microvascular channel completely inhibited IL-2–induced vascular leakage (Fig. 3A). Ang-1 also prevented paracellular gap formation even in the presence of 10% cyclic mechanical strain (Fig. 3, B and C). The Ang-1 antagonist angiopoietin-2 (Ang-2) has been shown to destabilize the capillary barrier (*31*) and promote pulmonary edema during IL-2 therapy or sepsis (*28*, *29*). Consistent with these observations, we found that Ang-2 (100 ng/ml) also induced pulmonary vascular leakage in the lung-on-a-chip when it was infused into the microvascular channel, and that coadministration of Ang-1 blocked this effect (Fig. 3A).

Mechanical strain can activate TRPV4 ion channels, and stimulation of these channels has been shown to increase alveolar-capillary permeability and cause vascular leakage in the lung (*32*–*34*). Therefore, we reasoned that pharmaceutical inhibition of TRPV4 channels might possibly prevent the exacerbation of IL-2–induced permeability owing to physiological cyclic mechanical strain. To test this, we examined the effects of a newly developed TRPV4 channel blocker, GSK2193874 (GlaxoSmithKline) (*20*), on barrier permeability in our disease model. When administered intravascularly (through the microvascular channel, Fig. 1B), this compound completely inhibited the increase in vascular permeability induced by IL-2 in combination with 10% cyclic mechanical strain (Fig. 3D). These results closely match

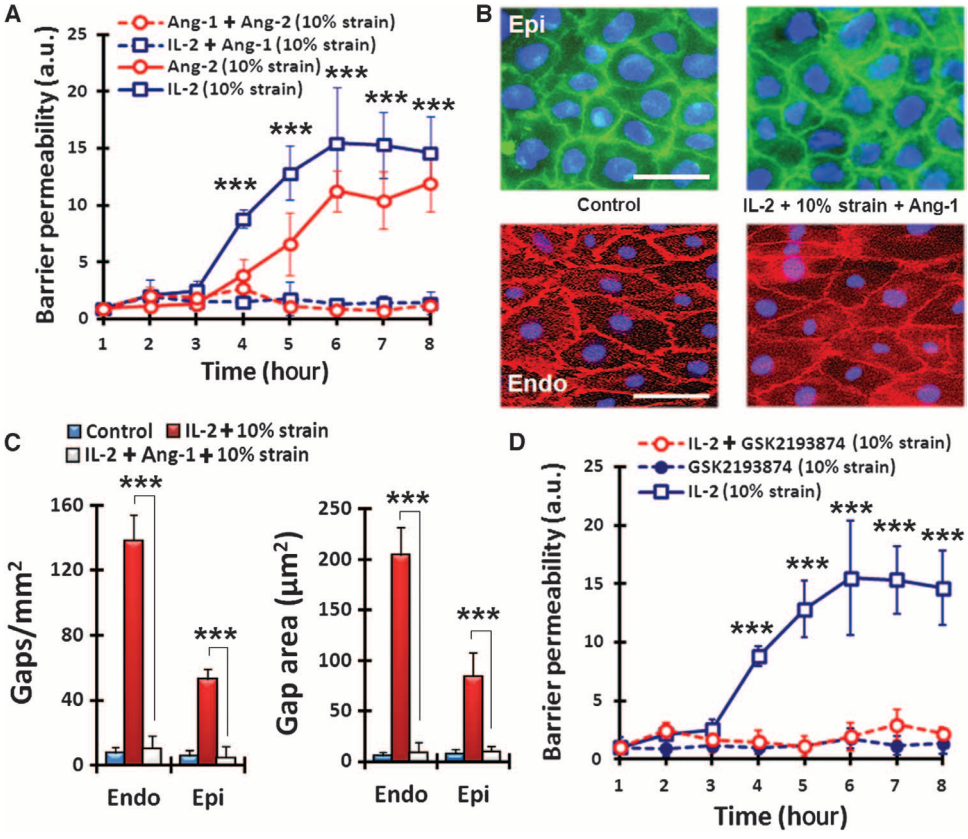

Fig. 3. Pharmacological modulation in lung-on-a-chip pulmonary edema model. (**A**) Administration of Ang-1 (100 ng/ml) prevents fluid leakage caused by IL-2 (1000 U/ml) and Ang-2 (100 ng/ml) applied in conjunction with mechanical stretch. Statistical significance was determined for comparison of IL-2 (10% strain) and IL-2 and Ang-1 (10% strain). (**B**) Immunostaining of epithelial occludin (green) and endothelial VE-cadherin (red) in cell-cell junctions after exposure to cyclic mechanical strain (10% at 0.2 Hz) without IL-2 (control) or with coadministration of IL-2 and Ang-1 for 3 days. Scale bars, 30 μm. (**C**) Restoration of barrier integrity by Ang-1 treatment assessed by changes in the number and size of intercellular gaps. ***$P < 0.001$. (**D**) Effect of the TRPV4 inhibitor GSK2193874 (100 nM) on barrier permeability, alone and in the presence of IL-2 and 10% strain. Statistical significance was determined for comparison of IL-2 alone and IL-2 with GSK2193874. (A, C, and E) Data are means ± SEM ($n = 3$). ***$P < 0.001$ (A, C, and E).

those obtained with the same TRPV4 inhibitor (GSK2193874) in rodent and canine models of pulmonary edema induced by heart failure (*20*), and the same study confirmed that cells of the human lung express TRPV4 channels.

Comparison of pulmonary edema-on-a-chip to whole mouse lung

To further investigate the physiological relevance of these results, we administered FITC-inulin and IL-2 intravenously to mice and analyzed alveolar-capillary barrier function in a whole-lung ex vivo ventilation-perfusion model (Fig. 4A). Fluorescence analysis of bronchoalveolar lavage samples collected from the whole lung confirmed that application of mechanical ventilation greatly accentuated the deleterious effect of IL-2 and increased barrier permeability by about threefold as compared with IL-2 administration without ventilation (Fig. 4B). These strain-induced changes were similar to the increases in permeability caused by physiological cyclic strain in our human pulmonary edema-on-a-chip (Fig. 4B). We also verified the ability of Ang-1 to prevent IL-2–induced fluid leakage into the lung in vivo, confirming the predictions made by our on-chip pulmonary edema model (Fig. 4B).

DISCUSSION

These data demonstrate the ability to leverage the unique capabilities of the human lung-on-a-chip microdevice to create a clinically relevant human disease model in vitro, ultimately to reliably predict drug toxicity and efficacy in humans. This on-chip pulmonary edema model effectively reproduces the intra-alveolar fluid accumulation, fibrin deposition, and impaired gas exchange that have been observed in living edematous lungs after 2 to 8 days of IL-2 therapy in humans (*23*). Using real-time, high-resolution imaging and quantitative analysis of barrier function, we discovered that physiological mechanical forces greatly exacerbate the detrimental effects of IL-2 treatment on both epithelial and endothelial tissue permeability. These studies provide new insight into the mechanism of IL-2–induced pulmonary edema by revealing that mechanical breathing motions increase permeability by increasing the size and number of gaps between cell-cell junctions in both the human pulmonary epithelium and endothelium in the presence of IL-2—a result that could not be readily examined in the animal models, nor can it be quantified easily in human biopsy specimens. IL-2–induced injury of the alveolar-capillary barrier in vivo is caused by apoptosis in both alveolar epithelial and pulmonary microvascular endothelial cells (*35*, *36*). Combined application of IL-2 and mechanical strain in the lung-on-a-chip might similarly trigger apoptosis in cultured cells, because this has been previously shown to destabilize cell-cell junctions and induce formation of intercellular gaps (*37*).

Recognition of the importance of this mechanical contribution also led to the identification of a potential new therapeutic agent that might be used to prevent IL-2–induced pulmonary toxicities. More specifically, GSK2193874, which inhibits TRPV4 channels that are activated by mechanical strain (*34*), prevented pulmonary edema induced by IL-2 in the lung-on-a-chip model. This result closely mimics in vivo results obtained with the same inhibitor in rodent and canine models of pulmonary edema induced by heart failure (*20*). This preclinical study by Thorneloe *et al.* serves to validate our findings and confirm the physiological relevance of the lung-on-a-chip model. Moreover, these studies together suggest that TRPV4 (and hence mechanical signaling) contributes to the development of cardiogenic (*20*) as well

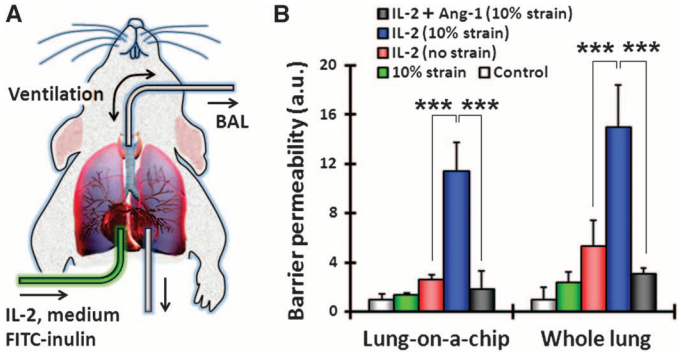

Fig. 4. Barrier permeability in the lung-on-a-chip compared to whole mouse lung ex vivo. (**A**) An excised whole mouse lung was mechanically ventilated ex vivo, and the pulmonary microvasculature was perfused with culture medium containing IL-2 (1000 U/ml) and FITC-inulin (1 mg/ml). After IL-2 treatment, bronchoalveolar lavage (BAL) fluid was collected for fluorescence measurement. (**B**) Barrier permeability was measured in the lung-on-a-chip and in the whole animal lung model. Control represents no strain and no IL-2. Data are means ± SEM (n = 3). ***P < 0.001.

as noncardiogenic (this study) forms of pulmonary edema. Thus, use of the biomimetic microdevice offers many unique capabilities that provide added value beyond what is available in current preclinical animal models.

Our studies also revealed that the pulmonary vascular leakage response elicited by IL-2 in this microsystem, which closely mimics the response seen in humans, does not require circulating immune cells. This finding is in contrast to previous in vitro and in vivo studies showing that blood-borne immune cells, such as lymphocytes and neutrophils, activated by IL-2 play a central role in the induction of pulmonary vascular leakage (*21*, *38*, *39*). Our results suggest that direct toxic effects of IL-2 on endothelial and epithelial cells, amplified by physiological forces, can mediate the onset and progression of IL-2–induced vascular injury and resultant pulmonary edema in the absence of immune cells. It is likely that the mechanically induced IL-2 toxicity might be further aggravated by recruitment of lymphocytes and neutrophils; however, future studies will be required to clarify whether and how particular immune cells contribute to this response. The human lung-on-a-chip system provides a robust means to address this question because it enables an investigator to introduce particular types of immune cells (one at a time or in combination) to determine their contributions. This is not currently possible with genetically engineered or irradiated animal models that are widely used to study the role of the immune system in pulmonary vascular leakage (*38*, *39*).

The finding that mechanical breathing motions exacerbate IL-2 toxicity and increase the likelihood of the development of pulmonary edema in this model system implies that reducing tidal volumes during mechanical ventilation, which is now standard of clinical care (*40*, *41*), also might be beneficial for minimizing pulmonary edema in patients on ventilators who receive IL-2 or exhibit symptoms of increased vascular leakage (for example, secondary to heart failure or sepsis). However, this requires further studies in animals and humans because we did not examine how different pressure waves or ventilation frequencies influence this response.

Recognition of the importance of mechanical forces for IL-2–induced pulmonary toxicity also led us to identify the TRV4 inhibitor GSK2193874 and Ang-1 as antagonists of intercellular gap formation and pulmonary vascular leakage caused by IL-2. These data suggest that these agents could represent potential new therapeutic agents for prevention of this life-threatening drug toxicity. These insights also might encourage the pharmaceutical industry to develop and screen for IL-2 replacements that produce their anticancer effects, without inducing these mechanosensitive toxic responses (and hence have fewer side effects). From a basic research perspective, it is also important to note that although the qualitative effects of IL-2, Ang-1, and Ang-2 on monolayer permeability can also be demonstrated under static culture conditions, the quantitative changes in vascular permeability induced by these agents in response to physiological breathing motions that we measured in vitro on-chip (and confirmed in vivo in whole mouse lung) could not be discovered under static culture conditions.

One potential limitation in these studies is that the pulmonary alveolar epithelial (NCI-H441) cells that we used were originally isolated from a lung tumor, and so they might not fully recapitulate critical barrier functions of the human alveolar epithelium in vivo. Addressing this question directly would require reproducing these experiments with primary human alveolar epithelial cells, but long-term culture of these primary human cells with maintenance of physiological barrier function and proliferative capacity in vitro has not yet been possible. The more important question, however, is whether our system recapitulates the critical pathological responses that are characteristic of pulmonary edema. The fact that our model mimics IL-2–induced pulmonary vascular leakage and clot formation at similar doses and time courses to those observed in humans clearly demonstrates that these transformed lung epithelial cells exhibit the critical subset of properties required to study key pulmonary disease processes and drug responses in vitro. We also previously showed that these cells reestablish pulmonary barrier functions that closely mimic those displayed in vivo when cultured in our lung chip device, whereas they do not in standard Transwell culture (*4*). Moreover, established cell lines that have the ability to mimic in vivo phenotypes, such as the one used in our studies, are much more robust than primary cells, which often can show unwanted batch-to-batch variability; this robustness makes them even more advantageous for technology translation and product development.

There are, however, still important physiological processes, such as reabsorption and clearance of fluid in the alveolar air space (*42*, *43*), that could be further studied to determine their relative contribution to development of pulmonary edema in this microengineered model system. For drug screening, the effects of serum-containing medium on test compounds also need to be explored in greater depth to ensure optimal evaluation and prediction of drug efficacy and toxicity on-chip.

In summary, analysis of this unique on-chip human disease model revealed three major new insights into the mechanism of IL-2–induced pulmonary edema: (i) Vascular leakage results from intercellular gap formation in both the epithelium and endothelium; (ii) mechanical breathing motions are a major contributor to IL-2–induced edema; and (iii) the onset and progression of pulmonary edema during IL-2 therapy do not require circulating immune cells. These findings suggest that a microengineered in vitro human disease model can potentially replace preclinical animal models of pulmonary edema currently used by the pharmaceutical industry to evaluate the effects of drugs on vascular leakage syndrome in the lung. Use of this microengineering

approach also allows one to develop the simplest model possible that retains physiological relevance and then to add complexity to the system as necessary, which is not possible in animal models. This in vitro organ chip platform might be applied to model diseases in other organs and to predict different drug efficacies and toxicities in humans. In this manner, human organ-on-chip disease models could provide a potential new approach to enhance our fundamental understanding of complex disease processes and to enable more rapid, accurate, cost-effective, and clinically relevant testing of drugs, as well as cosmetics, chemicals, and environmental toxins. On-chip human disease models also have the potential to facilitate the translation of basic discoveries into effective new treatment strategies.

MATERIALS AND METHODS

Device fabrication

The microfluidic devices used in this work were produced by the fabrication methods slightly modified from those that we reported previously (*4*). Briefly, the upper and lower layers of the microfluidic device were produced by casting poly(dimethylsiloxane) (PDMS) prepolymer against a photolithographically prepared master that contained a positive relief of parallel microchannels made of photoresist (SU8-50, MicroChem). The weight ratio of PDMS base to curing agent was 15:1. The cross-sectional size of the microchannels was 400 μm (width) × 100 μm (height) for the central culture channels and 200 μm (width) × 100 μm (height) for the side channels. Thin microporous PDMS membranes were generated by spin-coating PDMS prepolymer (15:1) at 2500 rpm for 10 min on a silanized PDMS (10:1) substrate and bringing the spin-coated PDMS layer in conformal contact with a photolithographically prepared master that had an array of 50-μm-tall circular posts. Pressure was applied constantly to the master during curing of PDMS to ensure intimate contact and penetration of posts through the spin-coated layer. This process produced 10-μm-thick PDMS membranes with circular through-holes. After being cured at 65°C overnight, the membrane surface was briefly treated with corona plasma generated by a handheld corona treater (Electro-Technic Products) and bonded to the upper PDMS substrate to achieve irreversible bonding between the layers. After overnight incubation at 65°C, the bottom surface of the membrane was treated with corona and permanently bonded to the lower PDMS layer after careful manual alignment.

The side chambers in the microfluidic device were created by etching the membrane layers in the side microchannels with tetrabutylammonium fluoride (TBAF) and *N*-methylpyrrolidinone (NMP) mixed at a volumetric ratio of 1:3 (TBAF/NMP). An etching solution was introduced into the side microchannels through inlet reservoirs by using hydrostatic pressure or vacuum suction at the outlet ports. The flow of etchant was driven at a constant flow rate of ~200 μl/min. The membrane layers containing pentagonal holes in the side channels completely etched away within 2 min. Etching continued until the thickness of the PDMS walls between the side chambers from the central culture channels became thinner than 30 μm. After etching, the side chambers were washed thoroughly with NMP for at least 3 min to remove any remaining PDMS etchant.

Microfluidic cell culture

Human pulmonary microvascular endothelial cells (Lonza) were cultured in EBM-2 medium supplemented with 5% fetal bovine serum (FBS) and growth factors according to the manufacturer's protocols. Alveolar epithelial cells (NCI-H441; American Type Culture Collection) were grown in RPMI 1640 supplemented with 10% FBS, L-glutamine (0.292 mg/ml), penicillin (100 U/ml), and streptomycin (100 μg/ml). The cells were maintained at 37°C in a humidified incubator under 5% CO_2 in air. Before cell seeding, microfluidic devices were sterilized by ultraviolet irradiation, and the porous membranes embedded in the central culture channels were coated with fibronectin (5 μg/ml in carbonate buffer). Alveolar epithelial cells were seeded into the upper channel at about 2×10^4 cells/cm^2 and allowed to attach to the membrane surface for 2 hours under static conditions. The attached cells were then perfused with culture medium by a syringe pump at a volumetric flow rate of 50 μl/hour. After 24 hours, the flow of culture medium was stopped, and the microfluidic device was inverted to seed endothelial cells onto the opposite side of the membrane.

After cell attachment, steady flows of culture media were driven in both the upper and lower channels at 50 μl/hour (fluid shear stress, ~0.2 dyne/cm^2). The cells in both microchambers were grown to confluence within 5 days. Once alveolar epithelial cells reached confluence, they were treated with culture medium containing 1 μM glucocorticoid dexamethasone (Sigma) to promote the formation of tight junctions (*44*). For air-liquid interface culture, culture medium was gently aspirated from the upper channel on day 5, and a 50:50 mixture of epithelial and endothelial medium was introduced into the lower channel to feed the alveolar epithelial cells on their basolateral side. The epithelial cells were grown at an air-liquid interface for 15 days. Microfluidic culture was maintained at 37°C in a humidified incubator with 5% CO_2 in air.

Mechanical stimulation

Before mechanical stretching, the outlet holes of the side chambers were blocked, and the inlet ports were connected to a computer-controlled vacuum pump via vacuum-resistant tubing. Cyclic stretching was achieved by applying vacuum to the two side chambers simultaneously in a cyclic fashion. To mimic physiological breathing motion, we stretched the alveolar-capillary barriers formed in the microfluidic device with 10% strain at a frequency of 0.2 Hz (sinusoidal wave form). Before experiments, cells were stretched for 3 days with the specified regimen.

Immunostaining

For staining of occludin, alveolar epithelial cells in the upper microchannel were washed with phosphate-buffered saline (PBS), fixed with 4% paraformaldehyde in PBS for 20 min, rinsed with PBS, and permeabilized with 0.5% Triton X-100 in PBS for 10 min. The cells were washed with PBS and blocked with 2% bovine serum albumin in PBS for 1 hour, then incubated with FITC-conjugated mouse anti-human occludin antibody (Invitrogen) for 1 hour and washed with PBS.

For staining of vascular endothelial cadherin (VE-cadherin), microvascular endothelial cells in the microfluidic device were fixed, permeabilized, and blocked following the same methods described above. The cells were then incubated with mouse anti-human VE-cadherin antibody for 1 hour and washed with PBS. Subsequently, Alexa 594–conjugated secondary antibody was added, and the cells were incubated for 1 hour before fluorescence imaging.

Permeability assay

The permeability of the alveolar-capillary barrier was assessed by measuring the rate of FITC-inulin transport from the lower microvascular

channel to the upper alveolar compartment. FITC-inulin (1 mg/ml in endothelial medium) was introduced into the lower channel, and inulin transport across the barrier was determined by serially sampling fluid from the upper channel and measuring its fluorescence intensity, which was used as an index of barrier permeability.

Oxygen transport measurements

Medium oxygenation was measured with an in-line fluorescent sensor off-chip (PreSens) before and after incubation of the device under 5% CO_2 in air at 37°C. Supplemented medium was deoxygenated by bubbling 95% N_2 and 5% CO_2 and infused into the device and sensors. Flow was regulated to 500 μl/hour with a syringe pump, and the O_2 concentrations measured in the first sensor before introduction into the microdevice were consistently below 2%; O_2 saturation levels were also measured after 20 min of perfusion through the lung chip at the outlet sensor. IL-2 was administered for 4 days to the device to induce fluid leakage into the air channel before initiating the experiment.

Ex vivo lung ventilation-perfusion experiments

All experimental animal protocols were approved by the Institutional Animal Care and Use Committee at Children's Hospital Boston and Harvard Medical School. Eight-week-old male C57BL/6 mice (The Jackson Laboratory) were weighed and then anesthetized with Avertin (200 mg/kg intraperitoneally). Ex vivo ventilation and perfusion of the mouse lung was facilitated by the IL-1 ex vivo mouse lung ventilation perfusion system (Harvard Apparatus). The trachea was incised via a surgical tracheotomy, and a 22-gauge stainless steel endotracheal tube was secured inside the trachea. The lungs were subsequently ventilated with a mouse ventilator (VCM-R, Hugo Sachs Elektronik) at a rate of 60 breaths/min, with a peak inspiratory pressure of 10 cm H_2O and a positive end expiratory pressure of 3 cm H_2O with compressed air.

After the initiation of mechanical ventilation, the chest was opened by thoracotomy, and heparin (100 IU) was injected into the right ventricle. After 30 s, the thoracic aorta and superior vena cava were cut, and the animal was exsanguinated. A suture was placed around the pulmonary artery and aorta. Flare-tipped cannulae custom-made with PE-90 tubing (0.86-mm internal diameter, 1.7-mm outer diameter; Becton Dickinson) were placed in the pulmonary artery and left atrium, and lungs were perfused with RPMI 1640 with 4% bovine albumin (probumin reagent grade), 0.7 g of NaCl/500 ml, and FITC-inulin (1 mg/ml) with a roller pump (ISM 834C, Ismatec SA) set at a constant flow rate of 0.5 ml/min in a recirculating system with a system volume of 6 ml. For 10 min after initiation of perfusion, the lungs were observed for leakage and/or obstruction to perfusion or airflow. If leakage or obstruction were observed, the experiment was aborted; if not, the initial 2 ml of perfusate, which contained residual blood cells and plasma, was discarded and not recirculated.

After the 10-min observation period, and depending on the experiment, IL-2 (1000 U/ml of recirculating perfusate) or carrier fluid (serving as a control) was injected into the reservoir containing the recirculating perfusion medium. Ang-1 was used at a concentration of 100 ng/ml of recirculating perfusate. The lungs were subsequently ventilated and perfused for 5 hours. Perfusate and lung temperatures were maintained at 37°C by housing the entire ex vivo ventilation perfusion system inside a standard cell incubator without CO_2 (Forma Scientific). Humidity was maintained in the range of 90 to 95%. Pulmonary arterial and left atrial pressures and airway flow and pressures were recorded with dedicated Type 379 vascular pressure and DLP2.5 flow and MPX Type 399/2 airway pressure transducers and TAM-A amplifiers (Hugo Sachs Elektronik). Vascular pressures were zeroed at the mid-lung level before each experiment and recorded with PolyVIEW16 software (Grass Technologies) running on a desktop PC running Windows XP SP2 (Microsoft Corporation). At the end of each experiment, the lungs were lavaged with 1.5 ml (500 μl × 3) of 0.9% normal saline, and the lavage fluid was stored at −20°C for later analysis.

Statistical analysis

Statistical significance was determined by analysis of variance (ANOVA) followed by post hoc Tukey's multiple comparison test.

SUPPLEMENTARY MATERIALS

www.sciencetranslationalmedicine.org/cgi/content/full/4/159/159ra147/DC1
Movie S1. Fluorescent fibrin clots in the alveolar microchannel of the human lung-on-a-chip.

REFERENCES AND NOTES

1. F. Pampaloni, E. G. Reynaud, E. H. Stelzer, The third dimension bridges the gap between cell culture and live tissue. *Nat. Rev. Mol. Cell Biol.* **8**, 839–845 (2007).
2. D. Huh, G. A. Hamilton, D. E. Ingber, From 3D cell culture to organs-on-chips. *Trends Cell Biol.* **21**, 745–754 (2011).
3. K. J. Jang, K. Y. Suh, A multi-layer microfluidic device for efficient culture and analysis of renal tubular cells. *Lab Chip* **10**, 36–42 (2010).
4. D. Huh, B. D. Matthews, A. Mammoto, M. Montoya-Zavala, H. Y. Hsin, D. E. Ingber, Reconstituting organ-level lung functions on a chip. *Science* **328**, 1662–1668 (2010).
5. P. J. Lee, P. J. Hung, L. P. Lee, An artificial liver sinusoid with a microfluidic endothelial-like barrier for primary hepatocyte culture. *Biotechnol. Bioeng.* **97**, 1340–1346 (2007).
6. J. H. Sung, M. L. Shuler, A micro cell culture analog (microCCA) with 3-D hydrogel culture of multiple cell lines to assess metabolism-dependent cytotoxicity of anti-cancer drugs. *Lab Chip* **9**, 1385–1394 (2009).
7. D. Huh, H. Fujioka, Y. C. Tung, N. Futai, R. Paine III, J. B. Grotberg, S. Takayama, Acoustically detectable cellular-level lung injury induced by fluid mechanical stresses in microfluidic airway systems. *Proc. Natl. Acad. Sci. U.S.A.* **104**, 18886–18891 (2007).
8. A. Grosberg, P. W. Alford, M. L. McCain, K. K. Parker, Ensembles of engineered cardiac tissues for physiological and pharmacological study: Heart on a chip. *Lab Chip* **11**, 4165–4173 (2011).
9. H. J. Kim, D. Huh, G. Hamilton, D. E. Ingber, Human gut-on-a-chip inhabited by microbial flora that experiences intestinal peristalsis-like motions and flow. *Lab Chip* **12**, 2165–2174 (2012).
10. K. Domansky, W. Inman, J. Serdy, A. Dash, M. H. Lim, L. G. Griffith, Perfused multiwell plate for 3D liver tissue engineering. *Lab Chip* **10**, 51–58 (2010).
11. N. J. Douville, P. Zamankhan, Y. C. Tung, R. Li, B. L. Vaughan, C. F. Tai, J. White, P. J. Christensen, J. B. Grotberg, S. Takayama, Combination of fluid and solid mechanical stresses contribute to cell death and detachment in a microfluidic alveolar model. *Lab Chip* **11**, 609–619 (2011).
12. Y. S. Torisawa, B. Mosadegh, T. Bersano-Begey, J. M. Steele, K. E. Luker, G. D. Luker, S. Takayama, Microfluidic platform for chemotaxis in gradients formed by CXCL12 source-sink cells. *Integr. Biol.* **2**, 680–686 (2010).
13. S. Chung, R. Sudo, P. J. Mack, C. R. Wan, V. Vickerman, R. D. Kamm, Cell migration into scaffolds under co-culture conditions in a microfluidic platform. *Lab Chip* **9**, 269–275 (2009).
14. K. E. Sung, N. Yang, C. Pehlke, P. J. Keely, K. W. Eliceiri, A. Friedl, D. J. Beebe, Transition to invasion in breast cancer: A microfluidic in vitro model enables examination of spatial and temporal effects. *Integr. Biol.* **3**, 439–450 (2011).
15. J. W. Song, S. P. Cavnar, A. C. Walker, K. E. Luker, M. Gupta, Y. C. Tung, G. D. Luker, S. Takayama, Microfluidic endothelium for studying the intravascular adhesion of metastatic breast cancer cells. *PLoS One* **4**, e5756 (2009).
16. E. D. Robin, C. E. Cross, R. Zelis, Pulmonary edema. 1. *N. Engl. J. Med.* **288**, 239–246 (1973).
17. E. D. Robin, C. E. Cross, R. Zelis, Pulmonary edema. 2. *N. Engl. J. Med.* **288**, 292–304 (1973).

18. J. V. Hurley, Current views on the mechanisms of pulmonary oedema. *J. Pathol.* **125**, 59–79 (1978).
19. L. B. Ware, M. A. Matthay, Clinical practice. Acute pulmonary edema. *N. Engl. J. Med.* **353**, 2788–2796 (2005).
20. K. S. Thorneloe, M. Cheung, W. Bao, H. Alsaid, S. Lenhard, M.-Y. Jian, M. Costell, K. Maniscalco-Hauk, J. A. Krawiec, A. Olzinski, E. Gordon, I. Lozinskaya, L. Elefante, P. Qin, D. S. Matasic, C. James, J. Tunstead, B. Donovan, L. Kallal, A. Waszkiewicz, K. Vaidya, E. A. Davenport, J. Larkin, M. Burgert, L. N. Casillas, R. W. Marquis, G. Ye, H. S. Eidam, K. B. Goodman, J. R. Toomey, T. J. Roethke, B. M. Jucker, C. G. Schnackenberg, M. I. Townsley, J. J. Lepore, R. N. Willette, An orally active TRPV4 channel blocker prevents and resolves pulmonary edema induced by heart failure. *Sci. Transl. Med.* **4**, 159ra148 (2012).
21. R. Baluna, E. S. Vitetta, Vascular leak syndrome: A side effect of immunotherapy. *Immunopharmacology* **37**, 117–132 (1997).
22. M. Rosenstein, S. E. Ettinghausen, S. A. Rosenberg, Extravasation of intravascular fluid mediated by the systemic administration of recombinant interleukin 2. *J. Immunol.* **137**, 1735–1742 (1986).
23. E. F. Conant, K. R. Fox, W. T. Miller, Pulmonary edema as a complication of interleukin-2 therapy. *AJR Am. J. Roentgenol.* **152**, 749–752 (1989).
24. E. Briasoulis, N. Pavlidis, Noncardiogenic pulmonary edema: An unusual and serious complication of anticancer therapy. *Oncologist* **6**, 153–161 (2001).
25. R. L. Kradin, L. A. Boyle, F. I. Preffer, R. J. Callahan, M. Barlai-Kovach, H. W. Strauss, S. Dubinett, J. T. Kurnick, Tumor-derived interleukin-2-dependent lymphocytes in adoptive immunotherapy of lung cancer. *Cancer Immunol. Immunother.* **24**, 76–85 (1987).
26. R. Satchi-Fainaro, R. Mamluk, L. Wang, S. M. Short, J. A. Nagy, D. Feng, A. M. Dvorak, H. F. Dvorak, M. Puder, D. Mukhopadhyay, J. Folkman, Inhibition of vessel permeability by TNP-470 and its polymer conjugate, caplostatin. *Cancer Cell* **7**, 251–261 (2005).
27. J. A. Bastarache, L. Wang, T. Geiser, Z. Wang, K. H. Albertine, M. A. Matthay, L. B. Ware, The alveolar epithelium can initiate the extrinsic coagulation cascade through expression of tissue factor. *Thorax* **62**, 608–616 (2007).
28. S. M. Parikh, T. Mammoto, A. Schultz, H. T. Yuan, D. Christiani, S. A. Karumanchi, V. P. Sukhatme, Excess circulating angiopoietin-2 may contribute to pulmonary vascular leak in sepsis in humans. *PLoS Med.* **3**, e46 (2006).
29. D. C. Gallagher, R. S. Bhatt, S. M. Parikh, P. Patel, V. Seery, D. F. McDermott, M. B. Atkins, V. P. Sukhatme, Angiopoietin 2 is a potential mediator of high-dose interleukin 2-induced vascular leak. *Clin. Cancer Res.* **13**, 2115–2120 (2007).
30. K. G. Peters, Vascular endothelial growth factor and the angiopoietins: Working together to build a better blood vessel. *Circ. Res.* **83**, 342–343 (1998).
31. P. C. Maisonpierre, C. Suri, P. F. Jones, S. Bartunkova, S. J. Wiegand, C. Radziejewski, D. Compton, J. McClain, T. H. Aldrich, N. Papadopoulos, T. J. Daly, S. Davis, T. N. Sato, G. D. Yancopoulos, Angiopoietin-2, a natural antagonist for Tie2 that disrupts in vivo angiogenesis. *Science* **277**, 55–60 (1997).
32. K. Hamanaka, M. Y. Jian, D. S. Weber, D. F. Alvarez, M. I. Townsley, A. B. Al-Mehdi, J. A. King, W. Liedtke, J. C. Parker, TRPV4 initiates the acute calcium-dependent permeability increase during ventilator-induced lung injury in isolated mouse lungs. *Am. J. Physiol. Lung Cell. Mol. Physiol.* **293**, L923–L932 (2007).
33. D. F. Alvarez, J. A. King, D. Weber, E. Addison, W. Liedtke, M. I. Townsley, Transient receptor potential vanilloid 4–mediated disruption of the alveolar septal barrier: A novel mechanism of acute lung injury. *Circ. Res.* **99**, 988–995 (2006).
34. C. K. Thodeti, B. Matthews, A. Ravi, A. Mammoto, K. Ghosh, A. L. Bracha, D. E. Ingber, TRPV4 channels mediate cyclic strain–induced endothelial cell reorientation through integrin-to-integrin signaling. *Circ. Res.* **104**, 1123–1130 (2009).
35. H. Guan, P. S. Nagarkatti, M. Nagarkatti, Blockade of hyaluronan inhibits IL-2-induced vascular leak syndrome and maintains effectiveness of IL-2 treatment for metastatic melanoma. *J. Immunol.* **179**, 3715–3723 (2007).
36. J. Zhang, R. J. Wenthold Jr., Z. X. Yu, E. H. Herman, V. J. Ferrans, Characterization of the pulmonary lesions induced in rats by human recombinant interleukin-2. *Toxicol. Pathol.* **23**, 653–666 (1995).
37. B. M. Corfe, C. Dive, D. R. Garrod, Changes in intercellular junctions during apoptosis precede nuclear condensation or phosphatidylserine exposure on the cell surface. *Cell Death Differ.* **7**, 234–235 (2000).
38. E. Assier, V. Jullien, J. Lefort, J. L. Moreau, J. P. Di Santo, B. B. Vargaftig, J. R. Lapa e Silva, J. Thèze, NK cells and polymorphonuclear neutrophils are both critical for IL-2-induced pulmonary vascular leak syndrome. *J. Immunol.* **172**, 7661–7668 (2004).
39. L. Melencio, R. J. McKallip, H. Guan, R. Ramakrishnan, R. Jain, P. S. Nagarkatti, M. Nagarkatti, Role of $CD4^+CD25^+$ T regulatory cells in IL-2-induced vascular leak. *Int. Immunol.* **18**, 1461–1471 (2006).
40. The Acute Respiratory Distress Syndrome Network, Ventilation with lower tidal volumes as compared with traditional tidal volumes for acute lung injury and the acute respiratory distress syndrome. *N. Engl. J. Med.* **342**, 1301–1308 (2000).
41. J. Lipes, A. Bojmehrani, F. Lellouche, Low tidal volume ventilation in patients without acute respiratory distress syndrome: A paradigm shift in mechanical ventilation. *Crit. Care Res. Pract.* **2012**, 416862 (2012).
42. L. B. Ware, M. A. Matthay, Alveolar fluid clearance is impaired in the majority of patients with acute lung injury and the acute respiratory distress syndrome. *Am. J. Respir. Crit. Care Med.* **163**, 1376–1383 (2001).
43. M. A. Matthay, H. G. Folkesson, C. Clerici, Lung epithelial fluid transport and the resolution of pulmonary edema. *Physiol. Rev.* **82**, 569–600 (2002).
44. M. I. Hermanns, R. E. Unger, K. Kehe, K. Peters, C. J. Kirkpatrick, Lung epithelial cell lines in coculture with human pulmonary microvascular endothelial cells: Development of an alveolo-capillary barrier in vitro. *Lab. Invest.* **84**, 736–752 (2004).

Acknowledgments: We thank M. Khan and D. Shea for assistance in device fabrication, T. C. Ferrante and M. Montoya-Zavala for confocal microscopy, and A. Bahinski for helpful discussions. **Funding:** This research was supported by funding from NIH/FDA (U01 NS073474-01) and DARPA (W911NF-12-2-0036) and by the Wyss Institute for Biologically Inspired Engineering at Harvard University. **Author contributions:** D.H. designed the research, performed the experiments with assistance from J.P.F. and G.A.H., analyzed the data, and wrote the manuscript. D.C.L. carried out the oxygen transport experiments with D.H. and analyzed the data. B.D.M. and S.J. established a whole mouse lung model and conducted animal studies in collaboration with D.H. K.S.T. and M.A.M. developed the TRPV4 inhibitor and assisted in the design of our studies using this compound. D.E.I. designed the research, analyzed the data, and helped to write the manuscript. **Competing interests:** The authors declare that they have no competing financial interests. Harvard University, Boston Children's Hospital, and the authors (D.E.I. and D.H.) have a patent related to this work: "Organ mimic device with microchannels and methods of use and manufacturing thereof" (U.S. patent pending). **Data and materials availability:** The GlaxoSmithKline (GSK) authors (K.S.T. and M.A.M.) will make available the TRPV4 inhibitor with a materials transfer agreement between the requestor and GSK.

Submitted 1 May 2012
Accepted 17 August 2012
Published 7 November 2012
10.1126/scitranslmed.3004249

Citation: D. Huh, D. C. Leslie, B. D. Matthews, J. P. Fraser, S. Jurek, G. A. Hamilton, K. S. Thorneloe, M. A. McAlexander, D. E. Ingber, A human disease model of drug toxicity–induced pulmonary edema in a lung-on-a-chip microdevice. *Sci. Transl. Med.* **4**, 159ra147 (2012).